



1 Evaluating the sensitivity of fine particulate matter (PM_{2.5}) simulations to chemical 2 mechanism in Delhi

3 Chinmay Jena^{1*}, Sachin D. Ghude^{1*}, Rachana Kulkarni¹, Sreyashi Debnath¹, Rajesh Kumar², Vijay Kumar
 4 Soni³, Prodip Acharja¹, Santosh H. Kulkarni⁴, Manoj Khare⁴, Akshara J. Kagainalkar⁴, Dilip M. Chate⁴, Kaushar
 5 Ali¹, Ravi S. Nanjundiah^{1,5}, Madhavan N. Rajeevan⁶

6 ¹Indian Institute of Tropical Meteorology, Ministry of Earth Sciences, India

7 ²National Center for Atmospheric Research, Boulder, CO, USA

8 ³India Meteorological Department, Ministry of Earth Sciences, New Delhi, India

9 ⁴Centre for Development of Advanced Computing (C-DAC), Pune, Maharashtra, India

10 ⁵Centre for Atmospheric and Oceanic Sciences, Indian Institute of Science, Bengaluru 560 012, India

11 ⁶Ministry of Earth Sciences, Prithvi Bhavan, Lodhi Road, New Delhi 110003, India

12 **Correspondence:** chinmayjena@tropmet.res.in, sachinghude@tropmet.res.in

13

14 Abstract

15 Elevated levels of fine particulate matter (PM_{2.5}) during winter-time have become one of the most important
 16 environmental concerns over the Indo-Gangetic Plain (IGP) region of India, and particularly for Delhi. Accurate
 17 reconstruction of PM_{2.5}, its optical properties, and dominant chemical components over this region is essential to
 18 evaluate the performance of the air quality models. In this study, we investigated the effect of three different
 19 aerosol mechanisms coupled with gas-phase chemical schemes on simulated PM_{2.5} mass concentration in Delhi
 20 using the Weather Research and Forecasting model with the Chemistry module (WRF-Chem). The model was
 21 employed to cover the entire northern region of India at 10 km horizontal spacing. Results were compared with
 22 comprehensive filed data set on dominant PM_{2.5} chemical compounds from the Winter Fog Experiment
 23 (WiFEX) at Delhi, and surface PM_{2.5} observations in Delhi (17 sites), Punjab (3 sites), Haryana (4 sites), Uttar
 24 Pradesh (7 sites) and Rajasthan (17 sites). The Model for Ozone and related Chemical Tracers (MOZART-4)
 25 gas-phase chemical mechanism coupled with the Goddard Chemistry Aerosol Radiation and Transport
 26 (GOCART) aerosol scheme (MOZART-GOCART) were selected in the first experiment as it is currently
 27 employed in the operational air quality forecasting system of Ministry of Earth Sciences (MoES), Government
 28 of India. Other two simulations were performed with the MOZART-4 gas-phase chemical mechanism coupled
 29 with the Model for Simulating Aerosol Interactions and Chemistry (MOZART-MOSAIC), and Carbon Bond 5
 30 (CB-05) gas-phase mechanism couple with the Modal Aerosol Dynamics Model for Europe/Secondary Organic
 31 Aerosol Model (CB05-MADE/SORGAM) aerosol mechanisms. The evaluation demonstrated that chemical
 32 mechanisms affect the evolution of gas-phase precursors and aerosol processes, which in turn affect the optical
 33 depth and overall performance of the model for PM_{2.5}. All the three coupled schemes, MOZART-GOCART,
 34 MOZART-MOSAIC, and CB05-MADE/SORGAM, underestimate the observed concentrations of major
 35 aerosol composition (NO₃⁻, SO₄²⁻, Cl⁻, BC, OC, and NH₄⁺) and precursor gases (HNO₃, NH₃, SO₂, NO₂, and O₃)
 36 over Delhi. Comparison with observations suggests that the simulations using MOZART-4 gas-phase chemical
 37 mechanism with MOSAIC aerosol performed better in simulating aerosols over Delhi and its optical depth over
 38 the IGP. The lowest NMB (-18.8%, MB = -27.4 µg/m³) appeared for the simulations using MOZART-MOSAIC



39 scheme, whereas the NMB was observed 32.5% ($MB = -47.5 \mu\text{g}/\text{m}^3$) for CB05-MADE/SORGAM and -53.3%
40 ($MB = -78 \mu\text{g}/\text{m}^3$) for MOZART-GOCART scheme.

41



42 1. Introduction

43 The industrial activities in India have escalated to new heights in the past three decades which
44 consequently have led to multiple urban environmental issues, especially deteriorating air quality due to
45 suspended particulate matter of aerodynamic diameter smaller than $2.5\ \mu\text{m}$ ($\text{PM}_{2.5}$) (Ghude et al., 2016; Ghude
46 et al., 2020). Therefore, it has become a matter of serious concern for public health in India. Currently, the air
47 quality in India, especially in the northern region of India in general and Delhi in particular, is among the
48 poorest in the world (World Health Organization, 2018). Therefore, managing air quality levels in this region of
49 India has emerged as a complicated task.

50
51 Recent studies indicate that the exposure to the exceptionally high level of outdoor $\text{PM}_{2.5}$ pollution in
52 the National Capital Region (NCR) Delhi poses a serious health risk to the public in Delhi (Ghude et al., 2016;
53 Guttikunda et al., 2013), particularly during the winter season. Diversity of emission sources (Chandra et al.,
54 2018; Hakkim et al., 2019), larger use of fossil fuel such as transport, industries, etc. (Chen et al., 2020), and
55 large scale intense open crop-residue burning in surrounding regions of Delhi (Jena et al., 2015a; Beig et al.,
56 2020; Kulkarni et al., 2020) is responsible for extreme air pollution episodes in the NCR region under
57 favourable meteorological conditions (Vadrevu et al., 2011; Gargava et al., 2015; Tiwari et al., 2018; Liu et al.,
58 2018; Krishna et al., 2019; Chate et al., 2013; Beig et al., 2013; Parkhi et al., 2016). This has drawn significant
59 academic and research interest in predicting high $\text{PM}_{2.5}$ levels using numerical air quality models (Guttikunda et
60 al., 2012; Beig et al., 2013; Krishna et al., 2019; Ghude et al., 2020; Kulkarni et al., 2020). Few recent studies
61 have tested the performance of air quality models, particularly WRF-Chem, in simulating hourly $\text{PM}_{2.5}$
62 concentrations in Delhi (Ojha et al., 2020; Chen et al., 2020; Ghude et al., 2020; Kulkarni et al., 2020). These
63 studies suggested that simulating and predicting extreme air quality episodes, particularly $\text{PM}_{2.5}$ concentrations
64 exceeding $300\ \mu\text{g}/\text{m}^3$, in the NCR region is a challenging task for the air quality models (Kumar et al., 2015;
65 Krishna et al., 2019; Bali et al., 2019). Large uncertainties are involved in the prediction of atmospheric
66 aerosols. This is because chemical transport models predictions suffer from errors in emission inventories (Jena
67 et al., 2015b), inadequate understanding of some of the processes (e.g., secondary organic aerosol formation)
68 (Balzarini et al., 2015), inaccuracies in the initialization of chemical and physical atmospheric state (Ghude et
69 al., 2020), systematic and random errors because of numerical approximations, and approaches the different
70 chemical mechanisms use to calculate size distribution of aerosols coupled with the gas-phase chemical
71 mechanism.

72
73 A recent study showed significant differences in simulating aerosol mass concentration over China
74 (Chen et al., 2016, 2017), Europe (Solazzo et al., 2012; Balzarini et al. 2015; Georgiou et al. 2018), USA
75 (Yahya et al., 2017; Hodzic et al., 2013) and Tibetan Plateau (Yang et al., 2018). Differences in the chemical
76 mechanism (Knote et al., 2015), parameterization of heterogeneous formation of secondary inorganic aerosols
77 (SIA), and secondary organic aerosols (SOA), which affects the aerosol process and the evolution of gas-phase
78 precursors, are found to play a key role in the reconstruction of aerosols in above studies. For organic aerosols,
79 the complexity of secondary formation and its aging processes and the lack of emission estimates of
80 intermediate-volatility and semi-volatile organic compounds affect the model performance (Chen et al., 2017;
81 Tsigaridis et al., 2014). Balzarini et al. (2015) showed that simulated total PM mass concentrations, as well as



aerosol subcomponents, vary between the RADM2 gas-phase chemical mechanism with Modal Aerosol Dynamics Model for Europe/Secondary Organic Aerosol Model (MADE/SORGAM) and CBMZ gaseous parameterization with Model for Simulating Aerosol Interactions and Chemistry (MOSAIC) aerosol mechanisms, and CBMZ-MOSAIC performed better in reproducing lower aerosol concentration than RADM2-MADE-SORGAM. Yang et al., (2018) also reported that RADM2-MADE/SORGAM could simulate higher surface $PM_{2.5}$ mass concentrations better than the CBMZ-MOSAIC module over the Tibetan Plateau because of the difference in aerosol compounds and distribution of computed aerosol concentrations between modes and bins. On the other hand, Georgiou et al. (2018) showed that simulated $PM_{2.5}$ by the RADM2-MADE/SORGAM mechanism exhibit lowest mean bias when compared to observations, but it overestimates the ammonium and sulfate aerosols. On the other hand, the MOSAIC aerosol mechanism overestimates $PM_{2.5}$ mass concentrations substantially over the eastern Mediterranean region. In a recent study, Curi et al., (2015) showed that magnitude of the uncertainties in AOD arising from the assumptions of aerosol mixing state (external, internal homogeneous, and internal core shell), the chemical species density, the species complex refractive index, and the hygroscopic growth factors is significant if compared with typical differences found in comparison of simulated values with AOD observations.

Most of these studies focused over the USA, Europe, or China. However, a detailed evaluation of $PM_{2.5}$ with different coupled chemical schemes (gas-phase mechanism with aerosol schemes) over the IGP region in general and Delhi in particular with scarce datasets left unclear view of WRF-Chem's ability to predict $PM_{2.5}$ over this region, a region documented to be one of the most polluted regions in South Asia. A very limited number of modelling studies have focused on evaluating the performance of the air quality models in simulating $PM_{2.5}$ mass concentration in Delhi on an hourly time scale during winter-time pollution. For example, Krishna et al., (2019); Ghude et al., (2020); Kulkarni et al., (2020) carried out WRF-Chem simulations over Delhi with MOZART-4 gas-phase chemistry and Goddard Chemistry Aerosol Radiation and Transport (GOCART) aerosol mechanism. They found that the model very well captures the temporal variation in $PM_{2.5}$ mass concentration driven by synoptic-scale meteorological variability, but shows substantial error in simulating the $PM_{2.5}$ magnitude and large model-observations differences. It is therefore important to evaluate the model capability in simulating the concentration of major $PM_{2.5}$ components and major oxidants and how different chemical mechanism affects the $PM_{2.5}$ mass concentrations over this region.

In this study, three two-month simulation experiments using Weather Research and Forecasting model with chemistry (WRF-Chem v3.9.1) were designed for the Northern region of India in general, and National Capital Region, Delhi in particular at 10 km grid resolution during winter-time. For this, we employ and inter-compare MOZART-GOCART, MOZART-MOSAIC, CB05-MADE/SORGAM coupled gas-phase chemistry and aerosol mechanisms to evaluate the simulated $PM_{2.5}$ mass concentrations with extensive ground-based observations in Delhi (17 sites), Punjab (3 sites), Haryana (4 sites), Uttar Pradesh (7 sites), and Rajasthan (17 sites). We also investigated the optical properties of aerosols, and ability of the different coupled chemical mechanism in the model to reconstruct the different aerosol components of $PM_{2.5}$ in Delhi using chemical speciation observations from the Winter Fog Experiment (WiFEX) that took place at the Indira-Gandhi International Airport, New Delhi (Ghude et al., 2017; Acharja et al., 2020). The comparison among the coupled



aerosol schemes aims at identifying the reasons for differences in model performance. Section 2 briefly describes the gas-phase chemistry and aerosol mechanisms used for the simulations, the basic model configuration, emission data used, and data used for the model evaluation. In section 3, we present the results from the sensitivity simulations and their evaluation with surface observations. Our conclusions and suggestions for further study are given in Section 4.

2. Model setup and description

In this study, we used the Weather Research and Forecasting model coupled with chemistry WRF-Chem v3.9.1 to simulate surface $PM_{2.5}$ mass concentration during the peak winter period, starting from 1 December 2017 to 31 January 2018. Recently, the model has been widely used to simulate the air quality in Delhi (Beig et al., 2013; Gupta and Mohan 2015; Ghude et al., 2020; Kulkarni et al., 2020; Chen et al., 2020) and to estimate NO_x and $PM_{2.5}$ mass concentration over India (Ghude et al., 2013; Krishana et al., 2019; Ojha et al., 2020; Beig et al., 2020). In this study, three sets of simulations were designed using following three widely used coupled schemes (gas-phase chemical mechanisms with aerosol schemes) to simulate the $PM_{2.5}$ mass concentrations over the northern region of India.

MOZART-GOCART (MG): In the first experiment, simulation is performed with the Model for Ozone and related Chemical Tracers (MOZART-4) gas-phase chemical mechanism (Emmons et al. 2010) coupled with the Goddard Chemistry Aerosol Radiation and Transport (GOCART) aerosol scheme (Chin et al., 2000; Ginoux et al., 2001). It includes 157 gas-phase reactions, 85 gas-phase species, 39 photolysis, and 16 bulk aerosol compounds. For this experiment, the chemistry scheme is consistent with the chemistry used in the global model that provides the chemical initial and boundary conditions. The GOCART aerosol model simulates five major types of aerosols, namely, sulfate, black carbon, organic carbon, dust, and sea salt. GOCART scheme does not simulate nitrate and secondary organic aerosols. The composition of GOCART aerosol module includes fine unspciated aerosol contribution (P_{25}), organic carbon (hydrophobic OC1 and hydrophilic OC2), organic black carbon (hydrophobic BC1 and hydrophilic BC2), sulfate (SO_4^{2-}), dust of different sizes (D_1 , D_2 , D_3 , D_4 and D_5 representing dust with effective radii of 0.5, 1.4, 2.4, 4.5 and 8 μm respectively), and sea salt of different sizes (S_1 , S_2 , S_3 and S_4 representing sea salt with effective radii of 0.3, 1.0, 3.25 and 5 μm respectively).

MOZART-MOSAIC (MM): In the second experiment, we used MOZART-4 gas-phase chemical mechanism coupled with the Model for Simulating Aerosol Interactions and Chemistry (MOSAIC) (Zaveri et al., 2008) aerosol scheme. MOSIAC includes sulfate ($SULF = SO_4^{2-} + HSO_4^-$), methanesulfonate ($CH_3SO_3^-$), ammonium (NH_4^+), sodium (Na), calcium (Ca), nitrate (NO_3^-), chloride (Cl^-), carbonate (CO_3), black carbon (BC), primary and organic mass (OC). Other unspecified inorganic species, inert minerals, and trace metals are lumped together as OIN (other inorganic mass). MOSIAC also allowed the gas-phase to partition to the particle-phase, which include H_2SO_4 , HNO_3 , HCl , NH_3 , and MSA (methanesulfonicacid), and also include secondary organic aerosols (SOA). MOSAIC uses a sectional aerosol bin approach for the representation of the aerosol size distribution. In the WRF-Chem model, one can choose between four and eight aerosol size bins, which are demarcated by their lower and upper dry particle diameters. In both cases, only one bin is assigned to aerosols with a diameter between 2.5 and 10 μm . Therefore, when four aerosol bins are used, three bins are assigned to



aerosols less than 2.5 μm in diameter. When eight aerosol bins are used, seven bins are assigned to aerosols with diameters within this range. Usually, it is sufficient to use the four-bin simulation option to which the focus is on air quality and it also reduces computational complexity (Georgiou et al., 2018).

CB05-MADE/SORGAM (CMS): In the third experiment, we conducted simulations using the Carbon Bond 5 (CB-05) gas-phase mechanism (Yarwood et al., 2005,) which includes 51 chemical species and 156 reactions. Aerosol processes are represented by the Modal Aerosol Dynamics for Europe/ Secondary Organic Aerosol Model (MADE/SORGAM) (Ahmadov et al., 2012) which uses modal aerosol size distribution, and includes an advanced secondary organic aerosol (SOA) treatment based on gas-particle partitioning and gas-phase oxidation in volatility bins. The CB05-MADE/SORGAM mechanism has also been coupled to existing model treatments of various feedback processes such as the aerosol semi-direct effect on photolysis rates of major gases and the aerosol indirect effect on cloud droplet number concentration and resulting impacts on shortwave radiation (Yahya et al., 2016).

The model domain covers the entire northern region of India at a horizontal grid spacing of 10 km and 47 vertical levels stretching from the surface to 10 hPa. Prior anthropogenic emissions of aerosols and trace gases ($\text{PM}_{2.5}$, PM_{10} , OC, BC, CO, NO_x , etc.) were taken from the EDGAR-HTAP (Emission Database for Global Atmos. Res. for Hemispheric Transport of Air Pollution) for the year 2010 at $0.1^\circ \times 0.1^\circ$ grid resolution and scaled to 2018 using scaling factors as given in Venkatraman et al. (2018). No diurnal variation was added to emissions. Biogenic emissions are calculated online using the Model of Emissions of Gases and Aerosols from Nature version 2.1 (MEGAN2.1) (Guenther et al., 2006) and dust emissions are based on the online Atmospheric and Environmental Research Inc. and Air Force Weather Agency (AER/AFWA) scheme (Jones and Creighton, 2011). Emissions from sea salt are generated based on the scheme of Gong et al. (1997). Daily open biomass burning emissions are obtained from the Fire INventory from NCAR (FINNv1.5) (<http://bai.acom.ucar.edu/Data/fire/>). The chemical initial and lateral boundary conditions come from the global model simulations from the Model for Ozone and Related Chemical Tracers (MOZART-4) and the meteorological initial and lateral boundary conditions are provided by National Centers for Environmental Prediction Final Reanalysis (NCEP/FNL) dataset, which is available every 6 hours. The simulations are reinitialized monthly to constrain meteorological fields toward NCEP/FNL reanalysis data while forwarding chemistry fields from the previous day. The details configuration of physics and chemistry options used in this study, as well as their corresponding references, can be found in Table S1.

2.1. Observational datasets and evaluation protocol

The surface $\text{PM}_{2.5}$ data used in this study are taken from the air quality monitoring network operated by the Indian Institute of Tropical Meteorology (IITM) and the Central Pollution Control Board (CPCB) in Delhi (17 sites), and CPCB monitoring network in Punjab (3 sites), Haryana (4 sites), Uttar Pradesh (7 sites), and Rajasthan (9 sites). The details of these monitoring locations are given in Table S2, and the geographical locations are shown in Figure 1. These sites are representative of traffic, airport, urban, and suburban areas. The quality control and assurance method, followed by CPCB for these air quality monitoring stations, is given at <https://cpcb.nic.in/quality-assurance-quality-control/>. Furthermore, we take the following steps to reassure the quality of $\text{PM}_{2.5}$ observations from the CPCB network stations. For Delhi data quality, we rejected all the



observations values below $10 \mu\text{g}/\text{m}^3$ and above $1500 \mu\text{g}/\text{m}^3$ at a given site if other sites in the network do not show values outside this range. The purpose of this step is to eliminate any short-term local influence that cannot be captured in the models and to retain the regional-scale variability. Second, we removed single peaks that are characterized by a change of more than $200 \mu\text{g}/\text{m}^3$ in just one hour for all the data in CPCB monitoring stations. This step filters random fluctuations in the observations. Third, we removed some very high $\text{PM}_{2.5}$ values that appeared in the time series right after the missing values. For any given day, we removed the sites from the consideration that either experience instrument malfunction and/or appear to be very heavily influenced by strong local sources. Measurement of the inorganic aerosol composition (chemical ions) CL^- , NO_3^- , SO_4^{2-} , and NH_4^+ are made using MARGA-2S instrument during 01 December 2017 to 31 January 2018 at Delhi as a part of the WiFEX field campaign at Delhi international airport (Ghude et al., 2017; Acharja et al., 2020). The quality assurance and control process applied to the measurement of the chemical ion is given at Acharja et al., (2020). The meteorological observation data used in this study are taken from the Indian Meteorological Department (IMD).

The focus of the model evaluation was mainly to assess whether the model is able to effectively reproduce the spatial and temporal distributions of ambient total $\text{PM}_{2.5}$ mass concentrations and key $\text{PM}_{2.5}$ aerosol composition in Delhi as compared to observations. WRF-Chem is currently employed in the operational air quality forecasting system of the Ministry of Earth Sciences (MoES), Government of India. It is therefore important to examine the performance assessment of WRF-Chem for air quality simulations on a regional scale in general and over Delhi in particular during heavy winter-time pollution. Statistical evaluation metrics such as mean bias (MB), Pearson's correlation coefficient (R), normalized mean bias (NMB), normalized mean error (NME) (the definition of those measures can be found in Yu et al., 2006, and Zhang et al., 2006), and index of agreement (IOA) ranging from 0 to 1 (Yahya et al., 2016) with a value of 1 indicating a perfect agreement, is used to evaluate the perforation of different sets of the experiment. For evaluation, the observational data are paired up with the simulated data on an hourly basis for each site, and then observational data and simulated data are averaged out for all sites in Delhi, Haryana, Uttar Pradesh, and Rajasthan. The statistics are then calculated based on the state-specific data pairs.

3. Results and discussion

3.1. Meteorological evaluation

To quantitatively evaluate the model performance for basic meteorological parameters, the data for the temperature at 2m (T_{2m}), relative humidity at 2m (RH_{2m}), and wind speed at 10m (WS_{10m}) from six stations over Delhi, India is used. Statistical metrics are derived by comparing the output of the three model simulations to hourly measurements averaged over all ground stations. Table 1 shows the correlation coefficient (r), mean bias (MB), and root mean squared error (RMSE) between observed and modeled temperature at 2m (T_{2m}), relative humidity at 2m (RH_{2m}), and wind speed at 10m (WS_{10m}) over Delhi, India. Modelled T_{2m} is in good agreement with observations ($\text{NMB} = 2$ to 5%) but shows higher RSME values (8.84 to 8.92°C) for all three mechanisms. The statistic for RH_{2m} indicates that the model has dry bias during winter for all the three mechanisms and model over-predicts WS_{10m} by an average of $\sim 1.2 \text{ ms}^{-1}$ for all three mechanisms. The over prediction of wind



236 speed and poor correlation could be due to the poor representation of surface drag exerted by the unresolved
 237 topography, other smaller-scale terrain features, and building morphology (Mar et al., 2016; Zhang et al., 2013).

238

239 3.2. Sensitivity simulation of different aerosol scheme

240 3.2.1. Fine particulate matter (PM_{2.5})

241 Figure 2 shows the comparison for temporal variation between observed and the modeled hourly PM_{2.5}
 242 mass concentrations from the sensitivity simulations with the three aerosol mechanisms from 1 December 2017
 243 to 31 January 2018 over Delhi. Observed (black) surface PM_{2.5} mass concentrations are averaged from the 17 air
 244 quality monitoring stations in Delhi, while simulated PM_{2.5} are for the MG (red), MM (blue), and CMS (green)
 245 experiments are averaged from the 17 grids containing these observation sites. It can be seen that the run with
 246 the MG, MM and CMS chemical schemes did not perform well, although it could capture the temporal variation
 247 associated with the synoptic-scale variability during the study period. The mean observed PM_{2.5} concentration
 248 during peak winter months was about 191 $\mu\text{g}/\text{m}^3$. Whereas, the mean modeled PM_{2.5} concentration vary from
 249 89.9 $\mu\text{g}/\text{m}^3$ with the MG mechanism to 163.8 $\mu\text{g}/\text{m}^3$ and 147.1 $\mu\text{g}/\text{m}^3$ with the MM and CMS mechanism
 250 respectively, showing a large variability in simulated PM_{2.5} in Delhi among these mechanisms. All three
 251 simulations with MG, MM and CMS chemical schemes significantly under-predict observed PM_{2.5}
 252 concentration averaged over Delhi. The statistic showed a large mean bias of about -101 $\mu\text{g}/\text{m}^3$ (RMSE = 146.3)
 253 for the simulation with the MG mechanism, which was about 53% of the corresponding observation. On the
 254 other hand, simulations with the CMS and MM mechanisms showed much better agreement. The performance
 255 statistic showed that the magnitude of bias decrease to -44 $\mu\text{g}/\text{m}^3$ (23%) and -27 $\mu\text{g}/\text{m}^3$ (14%) in the CMS and
 256 MM simulations, respectively. Differences between the MG, MM, and CMS simulation are more pronounced
 257 during the days when hourly PM_{2.5} exceeds 250 $\mu\text{g}/\text{m}^3$, particularly on 1-7 and 25-31 December 2017, and 17-20
 258 January 2018. Simulations with the MG mechanisms show poor ability of the model to capture these heavy
 259 pollution days, while the latter two show reasonable ability to capture hourly PM_{2.5} that exceeds 250 $\mu\text{g}/\text{m}^3$. On
 260 some days, none of the simulation experiments captured the abrupt increase in PM_{2.5} values observed on 18-23
 261 December, 26-28 December, and 8-16 January and underestimated the observed levels at the majority of the
 262 stations.

263 Further, we evaluated the robustness of model performance for the individual stations in NCR Delhi
 264 region. Table S3 shows the statistical performance of three MG, MM and CMS chemical schemes for seventeen
 265 stations. Again, the MG mechanism showed the poorest performance with model mean bias varying from 19%
 266 to 65% among different stations. The statistics show that for some stations, the MM mechanism performed quite
 267 well, while the CMS mechanism shows better agreement for the others (Table S3). Surface PM_{2.5} concentration
 268 simulated with the MM mechanism show normalized mean bias (NMB) within $\pm 15\%$ for the following sites:
 269 CRRI Mathura (-1.9%), ITO (-7.3%), Lodhi Road (-4.8%), North Campus DU (-12.6%), and Shadipur (-
 270 11.5%). The sites showing the NMB within $\pm 15\%$ for the CMS mechanism are Burari Crossing (-11.51%),
 271 CRRI Mathura (-7.3%), ITO (-12.1%), and Lodhi Road (-2.1%). Overall, the MM mechanism shows better
 272 performance for simulating hourly PM_{2.5} mass concentration over individual stations and Delhi as a whole, but



both the MM and CMS mechanisms show significant variability in NMB among the monitoring stations. This could be because of the anthropogenic emissions of aerosols and trace gases taken from the EDGAR- HTAP at $0.1^\circ \times 0.1^\circ$ grid resolution, which does not resolve the real variability in emissions in Delhi and may not accurately capture true values observed at the point of measurement. Simulations with the MG mechanism under-predicts $PM_{2.5}$ within 70% at all stations, possibly due to lack of NO_3^- and secondary organic aerosols (SOA) in the GOCART model. We find that simulated mean NO_3^- and SOA together contributed $\sim 44 \mu g/m^3$ with the MM mechanism, which is about 30% of total $PM_{2.5}$ mass concentration simulated during the winter period.

We also examined the model performance of MG, MM and CMS chemical schemes over the Punjab, Haryana, Uttar Pradesh, and Rajasthan (Figure 3), which are the neighboring states of Delhi and often influences the air quality in NCR region (Kumar et al., 2015; Kulkarni et al., 2020). Table S4 shows the summary of the performance statistic for the individual sites in each state. The average observed $PM_{2.5}$ concentration over Punjab was $84.21 \mu g/m^3$ and WRF-Chem showed biases of about $-24.7 \mu g/m^3$ (RMSE = 52.1), $13.1 \mu g/m^3$ (RMSE = 52.6) and $1.9 \mu g/m^3$ (RMSE = 48.1) for the MG, MM, and CMS aerosol mechanisms respectively. This is about 29%, 15%, and 2% of the observed average value for the MG, MM, and CMS mechanisms, respectively. For the individual monitoring stations in Punjab, simulations with the CMS mechanism showed better performance with a bias of about 5.3% for Amritsar and 9.4% for Ludhiana, whereas the MM mechanism showed better performance with a bias of about -4.8% for Gobindgarh RIMT station.

The average observed $PM_{2.5}$ concentration over Haryana was about $138.8 \mu g/m^3$, significantly higher (by 45%) than that of average $PM_{2.5}$ over Punjab. WRF-Chem over Haryana showed a bias of about $-82.7 \mu g/m^3$ (-59.6%), $-43.7 \mu g/m^3$ (-31.5%) and $-58.9 \mu g/m^3$ (-42.4%) for the MG, MM and CMS chemical mechanisms respectively, indicating that all three aerosol mechanisms significantly under-predict $PM_{2.5}$ surface concentration. For the individual monitoring stations in Haryana, simulations with the MM mechanism showed better performance, and NMB is found to vary from -22% to 48% relative to observations. For Uttar Pradesh, the MG mechanism showed the largest bias of about $-126.5 \mu g/m^3$ (-62.2% of the observed value) while the MM and CMS showed biases of about $-58.4 \mu g/m^3$ (-28.5%) and $-84.6 \mu g/m^3$ (-42.4%) respectively, indicating a large error in simulations irrespective of the mechanism used. For the individual monitoring stations in Uttar Pradesh, NMB with simulations with the MM mechanism found to vary from -21% to 63% relative to observations. Relative to Haryana and Uttar Pradesh, performance statistics for Rajasthan show better results in terms of bias for MM mechanism (bias = $-7.6 \mu g/m^3$, NMB = -8.1%). Other two chemical mechanisms, MG and CMS, showed biases of about $-43.1 \mu g/m^3$ (-46%) and $-22.3 \mu g/m^3$ (-24%), respectively. Overall, all three MG, MM and CMS chemical mechanisms tend to underpredict the observed $PM_{2.5}$ concentration over the majority of stations in northern India, but the MM mechanism was found to be performing better over Delhi and neighbouring states, except Punjab, where the CMS mechanism performs the best.



3.2.2. Comparison with satellite AOD

We further examined how the differences between coupled chemical mechanisms translate in simulating Aerosol Optical Depth (at 550 nm) over the model domain. Figure 4 shows the spatial distribution of observed mean AOD (MODIS/TERRA) and simulated AOD at TERRA overpass time with three aerosol mechanisms. All three mechanisms under-predict the observed AOD, and the difference between the three mechanisms is more pronounced over the central and eastern regions of IGP. The mean AOD difference was the highest (-58%) for the simulation with MG mechanism, while the latter two show reasonably good agreement with a mean bias of about -4.3% and -6.6% for the MM and CMS mechanism. This indicates the crucial role of the fine particle of aerosols, which have higher scattering efficiency, in aerosol optical depth budget (Seinfeld et al., 2016; Balzarini et al. 2015; Yang et al., 2018). In spite of good agreement with mean AOD, simulations with both the MM and CMS mechanisms show still large bias over the central and eastern regions of IGP compared to other regions in the model domain. With the simulation with MG mechanism, the difference in magnitude between observed and modelled AOD vary from -0.6 to -0.8 over this region. The observed differences between simulated and observed AOD values over this region are consistent with results from previous studies (Kulkarni et al., 2020 and Nair et al., 2012). These studies found that underestimation of anthropogenic emissions in the IGP and errors in simulating dust emission and transport over this region are some of the reasons for differences in observed and modelled AOD. However, given that emissions are constant in all the three simulation experiments, the considerable differences between modelled and observed AOD might partially coming from the difference in the simulation of the aerosol composition and dust scheme. In our simulation, the MG and CMS use GOCART/AFWA dust scheme while MM uses the GOCART dust scheme. Some of the previous studies have shown that ammonium sulfate $((\text{NH}_4)_2\text{SO}_4)$, ammonium bisulfate $((\text{NH}_4)\text{HSO}_4)$, ammonium nitrate (NH_4NO_3) and ammonium chloride (NH_4Cl) scatter light more efficiently at 550 nm (Seinfeld et al., 2016), while BC absorbs the light at 550 nm. The spatial pattern of mean BC concentration and concentrations of gas-phase compounds that lead to secondary inorganic aerosols and distribution of secondary aerosols for the three aerosol mechanisms is shown in Figure 5. We can see that the mean SO_4^{2-} (Figure 5h) was generally lower in the MG experiment and highest in the CMS experiment, particularly over the IGP and northeastern India. This discrepancy may be related to less chemical aqueous-phase oxidation of SO_2 by H_2O_2 in MOZART-4 gas-phase scheme because all the experiment shares the same SO_2 emissions. H_2O_2 is an efficient oxidant of sulphuric compounds in clouds and fog. During peak winter months, widespread fog is often detected over the IGP region during early morning hours and persists till late early afternoon (Ghude et al., 2017; Jenamani et al., 2015). As shown in figure 5f, simulations with the MG and MM (MOZART-4 gas-phase chemistry) mechanism showed a higher concentration of H_2O_2 over IGP, suggesting inefficient oxidation of SO_2 compared to the CMS experiment. Figure 5i shows the surface NO_3^- concentration simulated by the MM and CMS mechanism. Since the MG mechanism does not simulate nitrate aerosols, NO_3^- from the MG experiment is not shown here. Mean NO_3^- concentration was generally higher in the MM experiment than in the CMS experiment, particularly the magnitude of NO_3^- over central and eastern IGP region is larger. Similarly, as shown in Figure 5j, the magnitude of mean NH_4^+ concentration was also higher in the MM experiment over central and eastern IGP. On the other hand, mean HNO_3 concentration was found highest in the MG experiment, followed by the CMS experiment, and the lowest was found in MM (Figure 5g) experiment. The highest HNO_3 concentration observed in the MG experiment is related to the efficient photochemical conversion of NO_2 and OH to gas-phase HNO_3 . However,



the lack of aerosol thermodynamics in the MG mechanism means that HNO_3 stays in the gas-phase and does not partition to particle-phase. The main precursor for NO_3 is HNO_3 , and the equilibrium between nitrate and HNO_3 , and gas-phase NH_3 and HNO_3 can convert to aerosol NH_4NO_3 . This indicates that the gas-particle partitioning from HNO_3 to NH_4NO_3 is more efficient in the MM experiment than in the CMS experiment. While, higher HNO_3 concentration in the CMS experiment than in the MM experiment may be related to higher surface NO_2 (Figure 5b) concentration due to an efficient O_3 - NO titration process that readily transforms to HNO_3 with the photochemical reaction between NO_2 and OH , but not sufficiently converting to aerosol NH_4NO_3 . The MM and CMS experiment show higher BC concentration than the MG experiment (Figure 5d), but OC concentration is higher in the MG experiment over the entire IGP region than the MM and CMS experiments (Figure 5e). Further simulated BC to OC ratios is higher in the MG experiment over the IGP, compared to the other two experiments. Few recent studies have shown the significant concentration of chloride ions (Cl^-) in the IGP region (Ghude et al., 2017) and correlation of NH_4^+ with Cl^- implied that sizeable fraction NH_4^+ with Cl^- occurred in NH_4Cl molecular form (Ali et al., 2019) through a gas-phase reaction between HCl and NH_3 (Du et al., 2010). The primary source of this chloride is winter-time biomass and trash burning that occurred widespread over the IGP region, but emissions of chloride from these sources are not provided to the model, and therefore, the MM and CMS simulations show negligible concentrations of Cl^- over the IGP (Figure not shown) region. The bias between observed and simulated AOD may partially be related to missing NH_4Cl aerosols in the simulations. Magnitude of the uncertainties in model AOD also arises from the assumptions of aerosol mixing state (external, internal homogeneous, and internal core-shell), the chemical species density, the species complex refractive index, and the hygroscopic growth factors. Recent study shows that uncertainties in model AOD due to above parameter is significant if compared with typical differences found in comparison of simulated values with AOD observations (Curi et al., 2015).

3.2.3. Major $\text{PM}_{2.5}$ speciation

Table 2 shows that all three chemical mechanisms underestimate $\text{PM}_{2.5}$ concentrations in Delhi. The lowest NMB appears for the MM mechanism (NMB = -18.8%, MB = -27.4 $\mu\text{g}/\text{m}^3$), whereas the NMB for the GM mechanism is -53.3% (MB = -78 $\mu\text{g}/\text{m}^3$) and -32.5% (MB = -47.5 $\mu\text{g}/\text{m}^3$) for the CMS mechanism. Box-whiskers' plot of observed $\text{PM}_{2.5}$ mass concentrations at IGI airport and its comparison with simulated $\text{PM}_{2.5}$ mass concentrations for the different aerosol mechanisms is given in Figure 6. For observations, the 25th and 75th percentile of $\text{PM}_{2.5}$ values were observed between 75 $\mu\text{g}/\text{m}^3$ and 190 $\mu\text{g}/\text{m}^3$, whereas 25th and 75th percentile of $\text{PM}_{2.5}$ for the MM, CMS, and MG chemical mechanisms was observed between 75 $\mu\text{g}/\text{m}^3$ and 150 $\mu\text{g}/\text{m}^3$, 60 $\mu\text{g}/\text{m}^3$ and 120 $\mu\text{g}/\text{m}^3$, and 50 $\mu\text{g}/\text{m}^3$ and 90 $\mu\text{g}/\text{m}^3$, respectively. Among the three sensitivity experiments, the median value of $\text{PM}_{2.5}$ for MM (100 $\mu\text{g}/\text{m}^3$) simulation was found closer to observation (120 $\mu\text{g}/\text{m}^3$). Overall, $\text{PM}_{2.5}$ mass concentration simulated with the MM mechanism was found to be in better agreement with observations.

In order to understand the individual components of $\text{PM}_{2.5}$ chemical species and examine the difference in behavior by the aerosol mechanism for Delhi, we examine separately the dominant aerosol species in $\text{PM}_{2.5}$



and gas-phase compounds that lead to secondary inorganic aerosols. Figure 6 presents the box-whiskers plot for components of $PM_{2.5}$ from the observations and simulated by the model for the different coupled aerosol mechanisms at Delhi during the study period. It should be noted that nitrate is absent in GOCART; therefore, ammonium and nitrate are not shown in Figure 6. The MG mechanism does not simulate NH_4 but multiplies sulfate by 1.375 to account for NH_4 mass in total $PM_{2.5}$ mass concentration. Observations at Delhi during the study period suggest that the ratio of NH_4 to sulfate is about 1.545 during the winter season, which is about 11% higher. Further, simulated mean sulfate aerosols (SO_4^{2-}) concentration was largely underestimated ($\sim 40 - 60\%$) by the model in all three experiments with bias ranging from $9 \mu g/m^3$ to $14 \mu g/m^3$ compared to the observations (Table 2). However, the gas-phase precursor (SO_2) of sulfate aerosol simulated by the model was found to be slightly overestimated by about 4 - 5 ppb in all the simulations. This implies that chemical aqueous-phase oxidation of SO_2 by H_2O_2 and a heterogeneous nucleation rate from sulphuric acid (H_2SO_4) is not efficiently simulated by all three mechanisms over Delhi during the winter period. Nitrate and sulfate interact with each other through thermodynamic equilibrium but depends upon the gas-phase ammonia concentrations. It can be seen that for NH_3 , the simulations with MM and MG mechanism slightly overestimate NH_3 by about 2 - 4 ppb, respectively. On the other hand, simulations with CMS mechanism underestimate NH_3 by about 8 ppb for the same ammonia emissions. However, ammonium aerosols are underestimated by both the simulations with CMS (MB = $-26.3 \mu g/m^3$) and MM (MB = $-24.8 \mu g/m^3$) mechanisms compared to observations ($\sim 34 \mu g/m^3$). Simulated mean nitrate concentration was generally higher in the MM (MB = $-7.6 \mu g/m^3$, NMB = $\sim 25\%$) experiment than in the CMS (MB = $-19.4 \mu g/m^3$, NMB = $\sim 62\%$) experiment compared to observation ($28 \mu g/m^3$) but both the experiment show nitrate is negatively biased. As discussed earlier, the main precursor for NO_3 is HNO_3 , and the equilibrium between nitrate, HNO_3 , and gas-phase NH_3 . It can be seen that simulations with the MM and CMS mechanisms highly underestimate the HNO_3 concentration during the winter period. Overall, the gas-particle partitioning from HNO_3 to ammonium nitrate is not efficient in the MM and CMS chemical mechanism. The difference between underestimation of simulated ammonium and nitrate aerosols in the MM and CMS experiments could be due to the differences in the different treatment of the gas-to-particle partitioning from the nitric acid to ammonium nitrate as a function of humidity (Balzarini et al., 2015; Georgiou et al., 2018). Simulations with the MM and CMS simulations highly underestimate chloride aerosol concentrations (by about $0.1 \mu g/m^3$) compared to observations ($25 \mu g/m^3$) due to the absence of anthropogenic chloride emissions. This indicates considerable uncertainty in the representation of tropospheric chloride emissions and chemistry that affects aerosol formation. Earlier studies have also shown significant enhancement in anthropogenic chloride (chemical tracer for garbage, plastics, and tires burning) during the peak winter season (Acharja et al., 2020; Ghude et al., 2017). During cold winter nights, open biomass burning occurs on the streets and numerous residential localities in the IGP. In the cold winter conditions, people burn wood, leaf litter, garbage, plastics, and tires, etc. as these are available almost free-of-cost as compared to clean energy sources for which one needs to pay. Compared to observations, organic carbon and black carbon is underestimated by all the three experiments. The lowest mean bias ($\sim -11 \mu g/m^3$, $\sim 45\%$) for BC is found for the simulations with MM and CMS mechanism, while the simulation with MG mechanism show $\sim 65\%$ bias ($\sim -16 \mu g/m^3$) with respect to the observed BC concentration. For OC the lowest mean bias ($\sim -9 \mu g/m^3$, $\sim 35\%$) appears for the MG mechanism, whereas mean bias was $\sim -12 \mu g/m^3$ ($\sim 45\%$) for MM mechanism, and $\sim -15 \mu g/m^3$ ($\sim 51\%$) for CMS mechanism. Because all the three experiments use the same emission sources, discrepancies between the



MG, MM, and CMS experiments could be partially attributed to differences treatment of aerosols calculations by the modal and sectional bin approach. The MOSAIC scheme in this study uses Zaveri et al. (2008) approach to divide aerosols into four bins, whereas the CMS scheme use Mozurkewich (1993) approach to divide aerosols into three modes.

4. Conclusion

In this study, we simulated atmospheric gases and aerosols using three WRF/Chem modelling configuration to investigate the effect of coupled gas-phase chemistry and aerosol mechanisms on the reproductions of aerosol concentrations and aerosol optical depth over the northern region of India for the winter period. Simulated results were compared with the air quality observational data from 17 sites in Delhi, 4 sites in Haryana, 7 sites in Uttar Pradesh, 9 sites in Rajasthan over North India. Further, the performance of MOZART-GOCART (MG), MOZART-MOSAIC (MM), and CB05-MADE/SORGAM (CMS) coupled gas-phase chemistry and aerosol mechanisms were investigated for Delhi for major $PM_{2.5}$ chemical species observed during WiFEX field campaign at IGI Airport, Delhi. Performance of the model for basic meteorological parameters indicates that WRF-Chem could capture 2 m temperature very well but overestimate the wind speed by about 1.2 ms^{-1} at Delhi and may be related to the limited representation of the topography by the model.

Overall, all three coupled chemical mechanisms tend to underpredict the observed $PM_{2.5}$ concentration over the majority of stations in northern India, but the MOZART-MOSAIC mechanism was found to be performing better over Delhi and neighbouring states. Surface $PM_{2.5}$ concentration simulated by the MOZART-MOSAIC and CB05-MADE/SORGAM chemical mechanism demonstrated relatively lower bias compared to MOZART-GOCART chemical mechanism. The model sufficiently captured the spatial distribution of mean AOD in all three simulations, but MOZART-GOCART highly underpredicts the observed AOD compared to the other two chemical mechanisms. This is partly due to the difference in aerosol compounds and particularly missing nitrate and secondary organic aerosols from the MOZART-GOCART mechanism. MOZART-MOSAIC and CB05-MADE/SORGAM mechanism underestimate ammonium, nitrate, sulfate, BC, and OC aerosol mass concentrations, and anthropogenic chloride is completely missing from the simulation. These fine mode aerosols scatter/absorbed light more efficiently at 550 nm (Seinfeld et al., 2016), and underestimation of these species in simulations MOZART-MOSAIC and CB05-MADE/SORGAM mechanisms is partly related to observed-modelled bias for surface $PM_{2.5}$ and AOD over the region. Observations in Delhi show a significant contribution of chloride aerosols in SOA, and missing sources of anthropogenic chloride emission lead to large-bias between model and observed chloride concentrations. This is found to be one of the contributing factors for observed discrepancies between surface $PM_{2.5}$ and AOD in all three experiments over the northern region of India. In summary, the result suggests considerable uncertainty in MOZART-GOCART, MOZART-MOSAIC, and CB05-MADE/SORGAM chemistry in the representation of aerosol chemical species and chemistry that affects the aerosol formation. This further implies that the under-prediction of $PM_{2.5}$ concentrations in all three chemical mechanisms is partially coming from the under-prediction of major aerosol species of fine particulate matter over IGI Airport, Delhi. Therefore, the selection of chemical mechanisms is a key aspect, and MOZART-



MOSAIC mechanism could perform better in reconstructing the AOD aerosols over the northern region of India and surface $PM_{2.5}$ over Delhi and neighbouring states.

Data availability

The $0.1^\circ \times 0.1^\circ$ emission grid maps can be downloaded from the EDGAR website on https://edgar.jrc.ec.europa.eu/htap_v2/index.php?SECURE=_123 per year per sector. The model data is available at Prithvi (IITM) super-computer and can be provided upon request to the corresponding author. Observational data on $PM_{2.5}$ measurements can be obtained from the CPCB website on <https://app.cpcbcr.com/ccr>.

Author contributions

All authors contributed to the research; CJ and SDG designed the research; CJ conducted the research; CJ and SDG wrote the paper; CJ performed the WRF/Chem model simulations; RK contributed to writing; SD, VKS, PA, SHK, MK, AJK, DMC, KA, RN, and MR formulated the research.

Competing interests

The authors declare that they have no conflict of interest.

Acknowledgment:

We acknowledge the use of surface $PM_{2.5}$ data from air quality monitoring network of the Central Pollution Control Board (CPCB), India. This work was supported by funding from the national monsoon mission project of the Ministry of Earth Sciences (MoES). The use of MODIS data provided by NASA Earth Observing System Data and Information System (EOSDIS). The emissions inventory for chemical species from the HTAP and EDGAR emissions for 2010. We would like to acknowledge high-performance computing support from Aditya and Pratyush provided by the Indian Institute of Tropical Meteorology, Pune. This work was supported by the National Supercomputing Mission (NSM) program grant to the authors at C-DAC, and we are grateful to the Executive Director and the Director-General of C-DAC.



496 **References:**

- 497
 498 Acharja, P., Ali, K., Trivedi, D. K., Safai, P.D., Ghude, S. D., Prabhakaran, T., Rajeevan, M.: Characterization
 499 of atmospheric trace gases and water soluble inorganic chemical ions of PM₁ and PM_{2.5} at Indira
 500 Gandhi International Airport, New Delhi during 2017–18 winter, *Science of the Total Environment*,
 501 729, 138800, 2020.
- 502 Ali, K., Acharja, P., Trivedi, D. K., Kulkarni, R., Pithani, P., Safai, P. D., Chate, D. M., Ghude, S.D., Jenamani,
 503 R.K., Rajeevan, M.: Characterization and source identification of PM_{2.5} and its chemical and
 504 carbonaceous constituents during Winter Fog Experiment 2015-16 at Indira Gandhi International
 505 Airport, Delhi, *Science of the Total Environment*, 662,, DOI:10.1016/j.scitotenv.2019.01.285, 687-696,
 506 2019.
- 507 Ahmadov, R., McKeen, S. A., Robinson, A. L., Bareini, R., Middlebrook, A. M., De Gouw, J. A., Meagher, J.,
 508 Hsie, E.-Y., Edgerton, E., Shaw, S., and Trainer, M.: A volatility basis set model for summertime
 509 secondary organic aerosols over the eastern United States in 2006, *J. Geophys. Res.* 117, D06301,
 510 <https://doi.org/10.1029/2011JD016831>, 2012.
- 511 Bali, K., Dey, S., Ganguly, D. and Smith, K. R.: Space-time variability of ambient PM_{2.5} diurnal pattern over
 512 India from 18-years (2000-2017) of MERRA-2 reanalysis data, *Atmos. Chem. Phys.*
 513 Discuss., <https://doi.org/10.5194/acp-2019-731>, 2019.
- 514 Balzarini, A., Pirovano, G., Honzak, L., Zabkar, R., Curci, G., Forkel, R., Hirtl, M., San José, R., Tuccella, P.,
 515 and Grell, G. A.: WRF-Chem model sensitivity to chemical mechanisms choice in reconstructing
 516 aerosol optical properties, *Atmos. Environ.*, 115, 604–619,
 517 <https://doi.org/10.1016/j.atmosenv.2014.12.033>, 2015.
- 518 Beig, G., Chate, D. M., Ghude, S. D., Mahajan, A.S., Srinivas, R., Ali, K., Sahu, S. K., Parkhi, N., Surendran,
 519 D., Trimbake, H. R.: Quantifying the effect of air quality control measures during the 2010
 520 Commonwealth Games at Delhi, India, *Atmospheric Environment*, 80, 455-463, 2013.
- 521 Beig, G., Sahu, S. K., Singh, V., Tikle, S., Sobhana, S. B., Gargeva, P., Krishna, K. R., Rathod, A., Murthy,
 522 B.S.: Objective evaluation of stubble emission of North India and quantifying its impact on air quality
 523 of Delhi, *Science of the Total Environment*, 709, 136126, 2020.
- 524 Chandra, B. P., Sinha, V., Hakkim, H., Kumar, A., Pawar, H., Mishra, A. K., Sharma, G., Garg, P. S., Ghude, S.
 525 D., Chate, D. M., Pithani, P., Kulkarni, R., Jenamani, R. K., Rajeevan, M., Odd-even traffic rule
 526 implementation during winter 2016 in Delhi did not reduce traffic emissions of VOCs, carbon dioxide,
 527 methane and carbon monoxide, *Curr. Sci.*, 114, 1318–1325, 2018.
- 528 Chate, D. M., Beig, G., Satpute, T., Sahu, S. K., Ali, K., Parkhi, N., and Ghude, S. D.: Assessments of
 529 population exposure to environmental pollutants using air quality measurements during
 530 Commonwealth Games-2010, *Inhalation Toxicol.*, 25, 333–340, 2013.
- 531 Chen, Y., Wild, O., Ryan, E., Sahu, S. K., Lowe, D., Scott A. -N., Wang, Yu., McFiggans, G., Ansari, T.,
 532 Singh, V., Sokhi, R. S., Archibald, A., and Beig, G.: Mitigation of PM_{2.5} and ozone pollution in Delhi:
 533 a sensitivity study during the pre-monsoon period, *Atmos. Chem. Phys.*, 20, 499–514,
 534 <https://doi.org/10.5194/acp-20-499-2020>, 2020.



- 535 Chen, Q., Fu, T.-M., Hu, J., Ying, Q., and Zhang, L.: Modelling secondary organic aerosols in China, *Natl. Sci.*
 536 *Rev.*, 4, 806-809, <https://doi.org/10.1093/nsr/nwx143>, 2017.
- 537 Chen, D., Liu, Z., Fast, J., and Ban, J.: Simulations of sulfate-nitrate-ammonium (SNA) aerosols during the
 538 extreme haze events over northern China in October 2014, *Atmos. Chem. Phys.*, 16, 10707-10724,
 539 <https://doi.org/10.5194/acp-16-10707-2016>, 2016.
- 540 Chin, M., Savoie, D. L., Huebert, B. J., Bandy, A. R., Thornton, D. C., Bates, T. S., Quinn, P. K., Saltzman, E.
 541 S., and De Bruyn, W. J.: Atmospheric sulfur cycle simulated in the global model GOCART:
 542 Comparison with field observations and regional budgets, *J. Geophys. Res.-Atmos.*, 105, 24689-24712,
 543 <https://doi.org/10.1029/2000JD900385>, 2000.
- 544 Curci, G., Hogrefe, C., Bianconi, R., Im, U., Balzarini, A., Baró, R., Brunner, D., Forkel, R., Giordano, L., Hirtl,
 545 M., Honzak, L., Jiménez-Guerrero, P., Knöbe, C., Langer, M., Makar, P.A., Pirovano, G., Pérez, J.L.,
 546 San José, R., Syrakov, D., Tuccella, P., Werhahn, J., Wolke, R., Žabkar, R., Zhang, J., Galmarini, S.:
 547 Uncertainties of simulated aerosol optical properties induced by assumptions on aerosol physical and
 548 chemical properties: An AQMEII-2 perspective, *Atmospheric Environment*, 115, 541-552,
 549 <https://doi.org/10.1016/j.atmosenv.2014.09.009>, 2015.
- 550 Emmons, L. K., Walters, S., Hess, P. G., Lamarque, J.-F., Pfister, G. G., Fillmore, D., Granier, C., Guenther,
 551 A., Kinnison, D., Laepple, T., Orlando, J., Tie, X., Tyndall, G., Wiedinmyer, C., Baughcum, S. L., and
 552 Kloster, S.: Description and evaluation of the Model for Ozone and Related chemical Tracers, version 4
 553 (MOZART-4), *Geosci. Model Dev.*, 3, 43-67, 2010.
- 554 Gargava, P., Rajagopalan, V.: Source apportionment studies in six Indian Cities drawing broad inferences for
 555 urban PM10 reductions, *Air Qual., Atmosphere Health*, 1-11, 2015.
- 556 Georgiou, George K., TheodorosChristoudias, YiannisProestos, JonildaKushta, PanosHadjinicolaou and Jos
 557 Lelieveld: Air quality modelling in the summer over the eastern Mediterranean using WRF-Chem:
 558 chemistry and aerosol mechanism intercomparison, *Atmos. Chem. Phys.*, 18, 1555-1571,
 559 <https://doi.org/10.5194/acp-18-1555-2018>, 2018.
- 560 GhudeS. D.,Pfister,G. G., Jena, C., van der A, R.J., Emmons,L. K., and Kumar,R.: Satellite constraints of
 561 nitrogen oxide (NOx) emissions from India based on OMI observations and WRF- Chem simulations,
 562 *Geophys. Res. Lett.*, vol. 40, 423-428, doi:10.1029/2012GL053926, 2013.
- 563 Ghude, S. D., Chate, D. M., Jena, C., Beig, G., Kumar, R., Barth,M. C., Pfister, G. G., Fadnavis, S., Rao, P.:
 564 Premature mortality in India due to PM_{2.5} and ozone exposure., *Geophys. Res. Lett.*, 43, 4650-4658,
 565 2016.
- 566 Ghude, S.D., Bhat G.S., Prabha T., Jenamani R.K., Chate D.M., Safai P.D., Karipot A.K., Konwar M., Pithani
 567 P., Sinha V., Rao P.S.P., Dixit S.A., Tiwari S., Todekar K., Varpe S., Srivastava A.K., Bisht D.S.,
 568 Murugavel P., Ali K., Mina U., Dharua M., Jaya Rao Y., Padmakumari B., Hazra A., Nigam N.,
 569 Shende U., Lal D.M., et.al., Acharja P., Kulkarni R., Subharthi C., Balaji B., Varghese M., Bera S. and
 570 M. Rajeevan, Winter fog experiment over the Indo-Gangetic plains of India, *Current Science*, 112, 767-
 571 784, doi:10.18520/cs/v112/i04/767-784, 2017.
- 572 Ghude, S. D., Kumar, R., Jena, C., Debnath, S., Rachana G. Kulkarni, Stefano Alessandrini, MrinalBiswas,
 573 SantoshKulkrani, PrakashPithani, SaurabKelkar, VeereshSajjan, D. M. Chate, V. K. Soni, Siddhartha
 574 Singh, Ravi S. Nanjundiah, and M. Rajeevan: Evaluation of PM2.5 forecast using chemical data



- 575 assimilation in the WRF-Chem model: a novel initiative under the Ministry of Earth Sciences Air
 576 Quality Early Warning System for Delhi, India, Current science (Accepted), 2020.
- 577 Ginoux, P., Chin, M., Tegen, I., Prospero, J. M., Holben, B., Dubovik, O., and Lin, S. J.: Sources and
 578 distributions of dust aerosols simulated with the GOCART model, J. Geophys. Res.-Atmos., 106,
 579 20255–20273, <https://doi.org/10.1029/2000JD000053>, 2001.
- 580 Gong, S., Barrie, L. A., and Blanchet, J. P.: Modeling sea salt aerosols in the atmosphere: 1. Model
 581 development, J. Geophys. Res., 102, 3805–3818, <https://doi.org/10.1029/96JD02953>, 1997.
- 582 Guenther, A., Karl, T., Harley, P., Wiedinmyer, C., Palmer, P. I., and Geron, C.: Estimates of global terrestrial
 583 isoprene emissions using MEGAN (Model of Emissions of Gases and Aerosols from Nature), Atmos.
 584 Chem. Phys., 6, 3181–3210, <https://doi.org/10.5194/acp-6-3181-2006>, 2006.
- 585 Gupta, M. and Mohan, M.: Validation of WRF-Chem model and sensitivity of chemical mechanisms to ozone
 586 simulation over megacity Delhi, Atmos. Environ., 122, 220–229,
 587 <https://doi.org/10.1016/j.atmosenv.2015.09.039>, 2015.
- 588 Guttikunda, S., Gurjar, B.: Role of meteorology in seasonality of air pollution in megacity Delhi, India,
 589 Environmental Monitoring and Assessment, 184, 3199–3211, 2012.
- 590 Guttikunda, S. K.; Goel, R.: Health impacts of particulate pollution in a megacity-Delhi, India, Environ. Dev., 6,
 591 8–20, 2013.
- 592 Hakkim, H., Sinha, V., Chandra, B. P., Kumar, A., Mishra, A., Sinha, B., Sharma, G., Pawar, H., Sohpaal, B.,
 593 Ghude, S. D., Pithani, P., Kulkarni, R., Jenamani, R. K., and Rajeevan, M.: Volatile organic compound
 594 measurements point to fog-induced biomass burning feedback to air quality in the megacity of Delhi,
 595 Science of the total environment, 295-304, <https://doi.org/10.1016/j.scitotenv.2019.06.438>, 2019.
- 596 Hodzic, A., Madronich, S., Aumont, B., Lee-Taylor, J., Karl, T., Camredon, M., Mouchel-Vallon, C.: Limited
 597 influence of dry deposition of semi-volatile organic vapors on secondary organic aerosol formation in
 598 the urban plume, Geophys. Res. Lett., 40, 3302-3307, doi:10.1002/grl.50611, 2013.
- 599 Jena, C., Ghude, S. D., Pfister, G. G., Chate, D. M., Kumar, R., Beig, G., Surendran, D. E., Fadnavis, S., and Lal,
 600 D. M.: Influence of springtime biomass burning in South Asia on regional ozone (O₃): A model based
 601 case study, Atmospheric Environment, 100, 37-47, 2014.
- 602 Jena, C., Ghude, S. D., Beig, G., Chate, D. M., Kumar, R., Pfister, G. G., Lal, D. M., Surendran, D. E., Fadnavis,
 603 S., van der A, R. J.: Inter-comparison of different NO_x emission inventories and associated variation in
 604 simulated surface ozone in Indian region, Atmospheric Environment, 117, 61-73, 2015.
- 605 Jenamani, R. K. and Rathod, L. S.: Physical processes from data analysis, real time fog forecast system,
 606 performances of various indigenous fog models and benchmarking. Technical Report (FDP-FOG 2008-
 607 2015), Meteorological Watch Office, IGI Airport, Delhi, 2015.
- 608 Jones, S. and Creighton, G.: AFWA dust emission scheme for WRF/Chem-GOCART, 2011 WRF workshop,
 609 20–24 June 2011, Boulder, CO, USA, 2011.
- 610 Knote, C., Tuccella, P., Curci, G., Emmons, L., Orlando, J. J., Madronich, S., Baró, R., Jiménez-Guerrero, P.,
 611 Lueken, D., Hogrefe, C., Forkel, R., Werhahn, J., Hirtl, M., Pérez, J. L., San José, R., Giordano, L.,
 612 Brunner, D., Yahya, K., Zhang, Y.: Influence of the choice of gas-phase mechanism on predictions of
 613 key gaseous pollutants during the AQMEII phase-2 intercomparison, Atmospheric Environment, 115,
 614 553-568, ISSN 1352-2310, <https://doi.org/10.1016/j.atmosenv.2014.11.066>, 2015.



- 615 Krishna, R. K., Ghude, S. D., Kumar, R., Beig, G., Kulkarni, R., Nivdange, S., Chate, D. M.: Surface PM_{2.5}
 616 estimate using satellite-derived Aerosol Optical Depth over India., *Aerosol Air Qual. Res.*, 19, 25–37,
 617 2019.
- 618 Kulkarni, S. H., Ghude, S. D., Jena, C., Karumuri, R. K., Sinha, B., Sinha, V., Kumar, R., Soni, V. K., and
 619 Khare, M.: How Much Does Large-Scale Crop Residue Burning Affect the Air Quality in Delhi?,
 620 *Environ. Sci. Technol.*, 54, 4790–4799, 2020.
- 621 Kumar, R., Barth, M. C., Pfister, G. G., Nair, V. S., Ghude, S. D., and Ojha, N.: What controls the seasonal
 622 cycle of black carbon aerosols in India?, *J. Geophys. Res. Atmos.*, 120, doi:10.1002/2015JD023298,
 623 2015.
- 624 Liu, L., Shawki, D., Voulgarakis, A., Kasoar, M., Samset, B.H., Myhre, G., Forster, P.M., Hodnebrog, Ø.,
 625 Sillmann, J., Aalbergstjø, S.G., Boucher, O., Faluvegi, G., Iversen, T., Kirkevåg, A., Lamarque, J.-F.,
 626 Olivie, D., Richardson, T., Shindell, D., and Takemura, T.: A PDRMIP multi-model study on the
 627 impacts of regional aerosol forcings on global and regional precipitation, *J. Climate*, 31, no. 11, 4429–
 628 4447, doi:10.1175/JCLI-D-17-0439.1, 2018.
- 629 Mar, K. A., Ojha, N., Pozzer, A., and Butler, T. M.: Ozone air quality simulations with WRF-Chem (v3.5.1)
 630 over Europe: model evaluation and chemical mechanism comparison, *Geosci. Model Dev.*, 9, 3699–
 631 3728, <https://doi.org/10.5194/gmd-9-3699-2016>, 2016.
- 632 Mozurkewich, M.: The dissociation constant of ammonium nitrate and its dependence on temperature, relative
 633 humidity and particle size, *Atmos. Environ. A-Gen.*, 27, 261–270, [https://doi.org/10.1016/0960-](https://doi.org/10.1016/0960-1686(93)90356-4)
 634 [1686\(93\)90356-4](https://doi.org/10.1016/0960-1686(93)90356-4), 1993.
- 635 Nair, V. S., Solomon, F., Giorgi, F., Mariotti, L., Babu, S. S., Moorthy, K. K.: Simulation of South Asian
 636 aerosols for regional climate studies, *J. Geophys. Res. Atmos.*, 117, No. D04209,
 637 <https://doi.org/10.1029/2011JD016711>, 2012.
- 638 Ojha, N., Sharma, A., Kumar, M., Girach, I., Ansari, T. U., Sharma, S. K., Singh, N., Pozzer, A., and Gunthe, S.
 639 S.: On the widespread enhancement in fine particulate matter across the Indo-Gangetic Plain towards
 640 winter, *Scientific Reports*, 10:5862, 2020.
- 641 Parkhi, N., Chate, D. M., Ghude, S. D., Peshin, S., Mahajan, A., Srinivas, R., Surendran, D., Ali, K., Singh, S.,
 642 Trimbake, H., Beig, G.: Large inter annual variation in air quality during the annual festival ‘Diwali’ in
 643 an Indian megacity, *Journal of environmental sciences*, 43, 265 – 272, 2016.
- 644 Seinfeld, J. H., Pandis, S. N., *Atmospheric Chemistry and Physics: From Air Pollution to Climate Change* (John
 645 Wiley & Sons, 2016).
- 646 Solazzo, E., Bianconi, R., Pirovano, G., Matthias, V., Vautard, R., Moran, M.D., Appel, K.W., Bessagnet, B.,
 647 Brandt, J., Christensen, J.H., Chemel, C., Coll, I., Ferreira, J., Forkel, R., Francis, X.V., Grell, G.,
 648 Grossi, P., Hansen, A.B., Miranda, A.I., Nopmongkol, U., Prank, M., Sartelet, K.N., Schaap, M., Silver,
 649 J.D., Sokhi, R.S., Vira, J., Werhahn, J., Wolke, R., Yarwood, G., Zhang, J., Rao, S.T., Galmarini, S.,
 650 Operational model evaluation for particulate matter in Europe and North America in the context of
 651 AQMEII, *Atmos. Environ.* 53, 75–92, <https://doi.org/10.1016/j.atmosenv.2012.02.045>, 2012.
- 652 Tiwari, S., Thomas, A., Rao, P., Chate, D.M., Soni, V. K., Singh, S., Ghude, S. D., Singh, D., Hopke, P. K.:
 653 Pollution concentrations in Delhi India during winter 2015–16: A case study of an odd-even vehicle
 654 strategy, *Atmospheric Pollution Research*, <https://doi.org/10.1016/j.apr.2018.04.008>, 2018.



- 655 Tsigaridis, K., Daskalakis, N., Kanakidou, M., Adams, P. J., Artaxo, P., Bahadur, R., Balkanski, Y., Bauer, S.
 656 E., Bellouin, N., Benedetti, A., Bergman, T., Bernsten, T. K., Beukes, J. P., Bian, H., Carslaw, K. S.,
 657 Chin, M., Curci, G., Diehl, T., Easter, R. C., Ghan, S. J., Gong, S. L., Hodzic, A., Hoyle, C. R., Iversen,
 658 T., Jathar, S., Jimenez, J. L., Kaiser, J. W., Kirkevåg, A., Koch, D., Kokkola, H., Lee, Y. H., Lin, G.,
 659 Liu, X., Luo, G., Ma, X., Mann, G. W., Mihalopoulos, N., Morcrette, J.-J., Müller, J.-F., Myhre, G.,
 660 Myriokefalitakis, S., Ng, N. L., O'Donnell, D., Penner, J. E., Pozzoli, L., Pringle, K. J., Russell, L. M.,
 661 Schulz, M., Sciare, J., Seland, Ø., Shindell, D. T., Sillman, S., Skeie, R. B., Spracklen, D., Stavrakou,
 662 T., Steenrod, S. D., Takemura, T., Tiitta, P., Tilmes, S., Tost, H., van Noije, T., van Zyl, P. G., von
 663 Salzen, K., Yu, F., Wang, Z., Wang, Z., Zaveri, R. A., Zhang, H., Zhang, K., Zhang, Q., and Zhang, X.:
 664 The AeroCom evaluation and intercomparison of organic aerosol in global models, *Atmos. Chem.*
 665 *Phys.*, 14, 10845–10895, <https://doi.org/10.5194/acp-14-10845-2014>, 2014.
- 666 Vadrevu, K. P., Ellicott, E., Badarinath, K. V. S., Vermote, E.: MODIS derived fire characteristics and aerosol
 667 optical depth variations during the agricultural residue burning season, north India, *Environ. Pollut.*,
 668 159, 1560–1569, 2011.
- 669 Venkataraman, C., Brauer, M., Tibrewal, K., Sadavarte, P., Ma, Q., Cohen, A., Chaliyakunnel, S., Frostad, J.,
 670 Klimont, Z., Martin, R. V., Millet, D. B., Philip, S., Walker, K., and Wang, S.: Source influence on
 671 emission pathways and ambient PM_{2.5} pollution over India (2015–2050), *Atmos. Chem. Phys.*, 18,
 672 8017–8039, <https://doi.org/10.5194/acp-18-8017-2018>, 2018.
- 673 Yahya, K., Wang, K., Campbell, P., Glotfelty, T., He, J., and Zhang, Y.: Decadal evaluation of regional climate,
 674 air quality, and their interactions over the continental US and their interactions using WRF/Chem
 675 version 3.6.1., *Geoscientific Model Development Discussions*, 8, 8, 6707–6756, doi: 10.5194/gmdd-8-
 676 6707-2015, 2016.
- 677 Yahya, K., Glotfelty, T., Wang, K., Zhang, Y., and Nenes, A.: Modeling regional air quality and climate:
 678 improving organic aerosol and aerosol activation processes in WRF/Chem version 3.7.1, *Geosci.*
 679 *Model Dev.*, 10, 2333–2363, 2017.
- 680 Yang, Junhua, Shichang Kang, Zhenming Ji and Deliang Chen: Modeling the Origin of Anthropogenic Black
 681 Carbon and Its Climatic Effect Over the Tibetan Plateau and Surrounding Regions, *Journal of*
 682 *Geophysical Research: Atmospheres*, 123, 671–692. <https://doi.org/10.1002/2017JD027282>, 2018.
- 683 Yarwood, G., Rao, S., Yocke, M., and Whitten, G. Z.: Final Report –Updates to the Carbon Bond Chemical
 684 Mechanism: CB05, Rep.RT-04-00675, 246 pp., Yocke and Co., Novato, Calif., 2005.
- 685 Yu, S., Eder, B., Dennis, R., Chu, S.-H., and Schwartz, S.: New unbiased symmetric metrics for evaluation of
 686 air quality models, *Atmos. Sci. Lett.*, 7, 26–34, 2006.
- 687 Zaveri, R. A., Easter, R. C., Fast, J. D., and Peters, L. K.: Model for Simulating Aerosol Interactions and
 688 Chemistry (MOSAIC), *Journal of Geophysical Research*, 113, <https://doi.org/10.1029/2007JD008782>,
 689 2008.
- 690 Zhang, Y., Liu, P., Pun, B., and Seigneur, C.: A comprehensive performance evaluation of MM5-CMAQ for
 691 summer 1999 Southern Oxidants Study Episode, Part-I: Evaluation Protocols, Databases and
 692 Meteorological Predictions, *Atmos. Environ.*, 40, 4825–4838,
 693 <https://doi.org/10.1016/j.atmosenv.2005.12.043>, 2006.



694 Zhang, Y., Sartelet, K., Wu, S.-Y., and Seigneur, C.: Application of WRF/Chem-MADRID and
695 WRF/Polyphemus in Europe – Part 1: Model description, evaluation of meteorological predictions, and
696 aerosol–meteorology interactions, Atmos. Chem. Phys., 13, 6807–6843, [https://doi.org/10.5194/acp-](https://doi.org/10.5194/acp-13-6807-2013)
697 13-6807-2013, 2013.

698

699

700

701

702



703 **FIGURE CAPTIONS:**

704 **Figure 1:** Geographical locations of air quality monitoring stations. Delhi stations are represented by blue
 705 circles; red circles represent stations in the states of Punjab, Haryana, Rajasthan, and Uttar Pradesh.

706 **Figure 2:** The time series of hourly $PM_{2.5}$ concentrations from the simulation of MOZART-GOCART (red),
 707 MOZART-MOSAIC (blue), and CB05-MADE/SORGAM (green) aerosol mechanism was compared with the
 708 air quality observation (black) from the CPCB data in Delhi region from 1 December 2017 to 31 January 2018.

709 **Figure 3:** The time series of hourly $PM_{2.5}$ concentrations from the simulation of MOZART-GOCART (red),
 710 MOZART-MOSAIC (blue), and CB05-MADE/SORGAM (green) aerosol mechanism was compared with the
 711 air quality observation (black) from CPCB data of Punjab, Haryana, Uttar Pradesh, and Rajasthan.

712 **Figure 4:** Spatial distribution of simulated AOD of CB05-MADE/SORGAM, MOZART-MOSAIC, MOZART-
 713 GOCART, and its difference with observed mean AOD from MODIS.

714 **Figure 5:** Spatial distribution of simulated surface SO_2 , NO_2 , Ozone, BC, OC, H_2O_2 , HNO_3 , SO_4^{2-} , NO_3^- , NH_4^+
 715 of CB05-MADE/SORGAM, MOZART-MOSAIC, MOZART-GOCART model.

716 **Figure 6:** Box-whisker plots of Nitrate (NO_3^-), Ammonium (NH_4^+), Chlorine (Cl), Organic Carbon (OC), Black
 717 Carbon (BC), Sulfate (SO_4^{2-}), HNO_3 , SO_2 , NH_3 , NO_2 , Ozone and $PM_{2.5}$ for the MOZART-GOCART (MG),
 718 MOZART-MOSAIC (MM), and CB05-MADE/SORGAM (CMS) mechanisms over IGI Airport, Delhi.

719

720

721



Table1. Pearson's correlation coefficient (R), mean bias (MB), and root mean squared error (RMSE) of hourly values of temperature at 2m, relative humidity at 2m, planetary boundary layer height, and wind speed at 10m for the MOZART-GOCART (MG), MOZART-MOSAIC (MM), and CB05-MADE/SORGAM(CMS) mechanisms averaged over all stations in Delhi.

State	Variables	MOZART-GOCART			MOZART-MOSAIC			CB05-MADE/SORGAM		
		MB	RMSE	R	MB	RMSE	R	MB	RMSE	R
Delhi	T _{2m}	0.78	8.92	0.23	0.39	8.84	0.24	0.31	8.91	0.23
	RH	-36.6	41.8	0.21	-36.4	41.6	0.20	-36.5	41.7	0.17
	Wind Speed (WS _{10m})	1.2	2.0	0.26	1.2	1.9	0.25	1.1	1.9	0.27

Table2: Index of Agreement (IOA), mean bias (MB), normalized mean bias (NMB), and root mean squared error (RMSE) of hourly values of PM_{2.5} for the MOZART-GOCART (MG), MOZART-MOSAIC (MM), and CB05-MADE/SORGAM (CMS) mechanisms over IGI Airport, Delhi.

State	Station	Variables	MOZART-GOCART				MOZART-MOSAIC				CB05-MADE/SORGAM			
			MB	NMB (%)	RMSE	IOA	MB	NMB (%)	RMSE	IOA	MB	NMB (%)	RMSE	IOA
Delhi	IGI Airport	SO ₄ ²⁻	-13.8	-66.7	21.2	0.36	-13.9	-66.9	19.9	0.43	-8.7	-42.3	18.9	0.48
		BC	-15.7	-68.4	20.8	0.46	-10.4	-45.1	18.2	0.52	-10.8	-47.1	18.3	0.52
		OC	-9.2	-35.3	13.1	0.51	-11.7	-44.8	15.3	0.46	-13.4	-51.3	16.5	0.44
		NH ₄ ⁺	-	-	-	-	-24.8	-73.8	30.2	0.44	-26.3	-78.1	31.5	0.43
		NO ₃ ⁻	-	-	-	-	-7.6	-25.8	18.8	0.45	-19.4	-62.4	24.7	0.41
		CL ⁻	-	-	-	-	-	-	-	-	-	-	-	-
		PM _{2.5}	-77.9	-53.3	102.7	0.53	-27.4	-18.8	81.2	0.69	-47.5	-32.5	86.5	0.66



Figure 1:

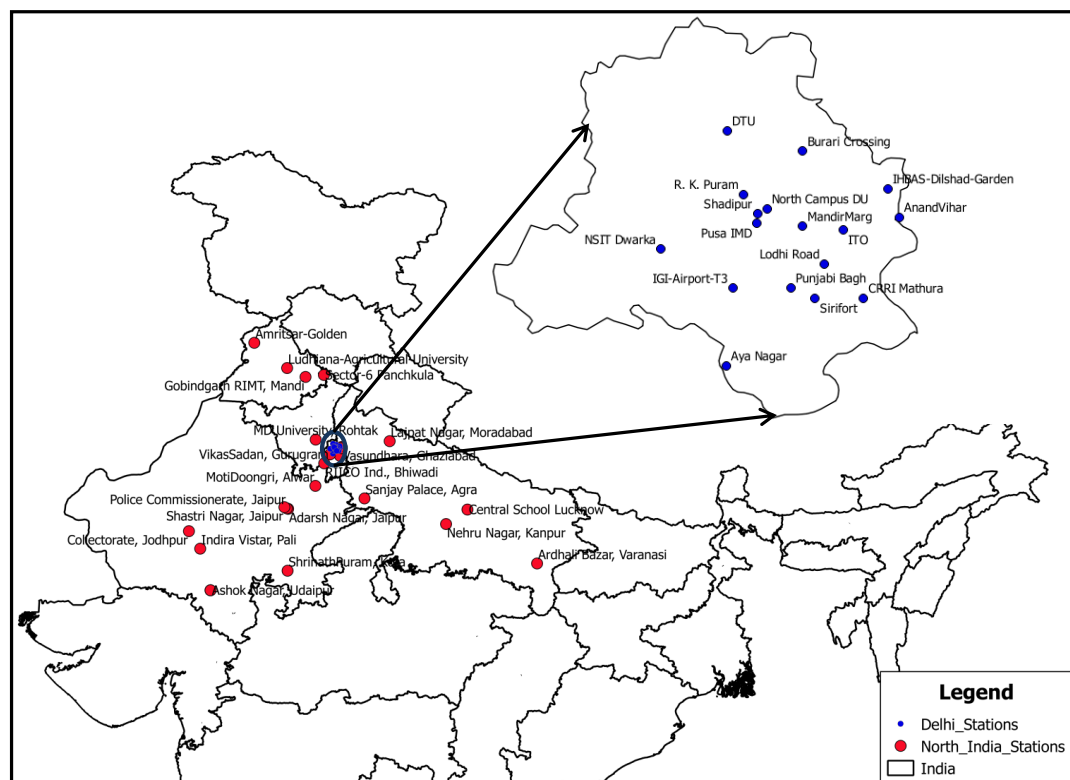




Figure 2 :

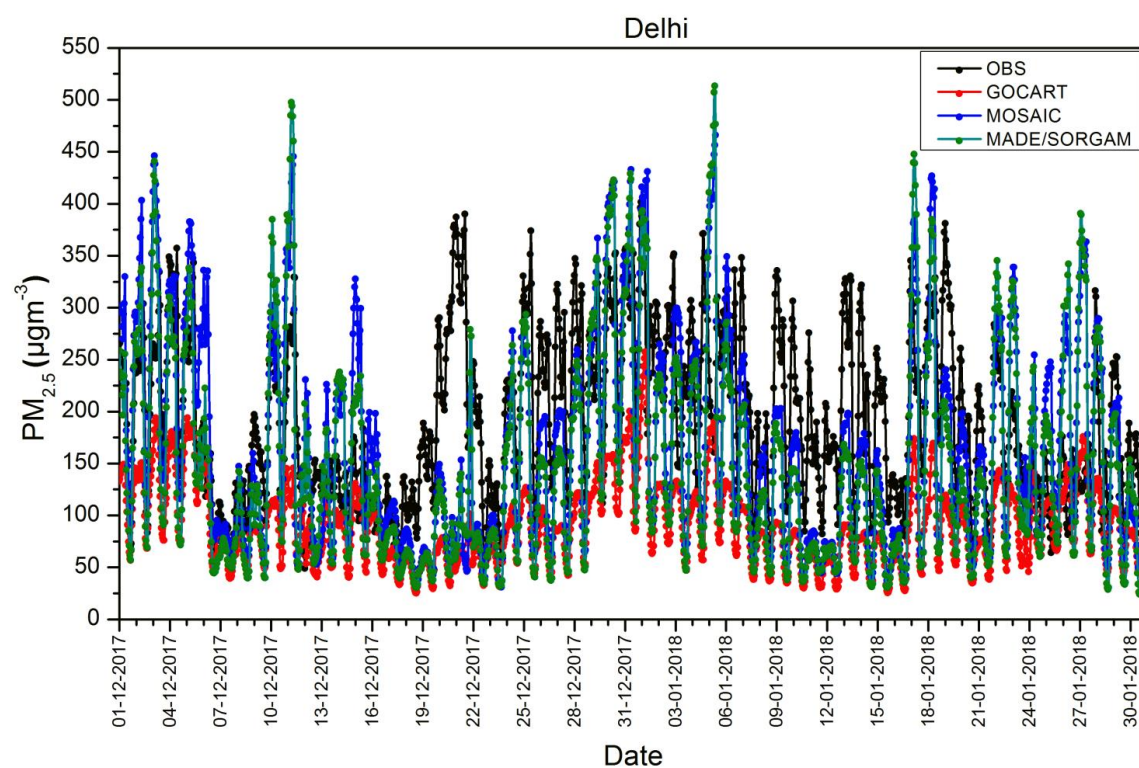




Figure 3:

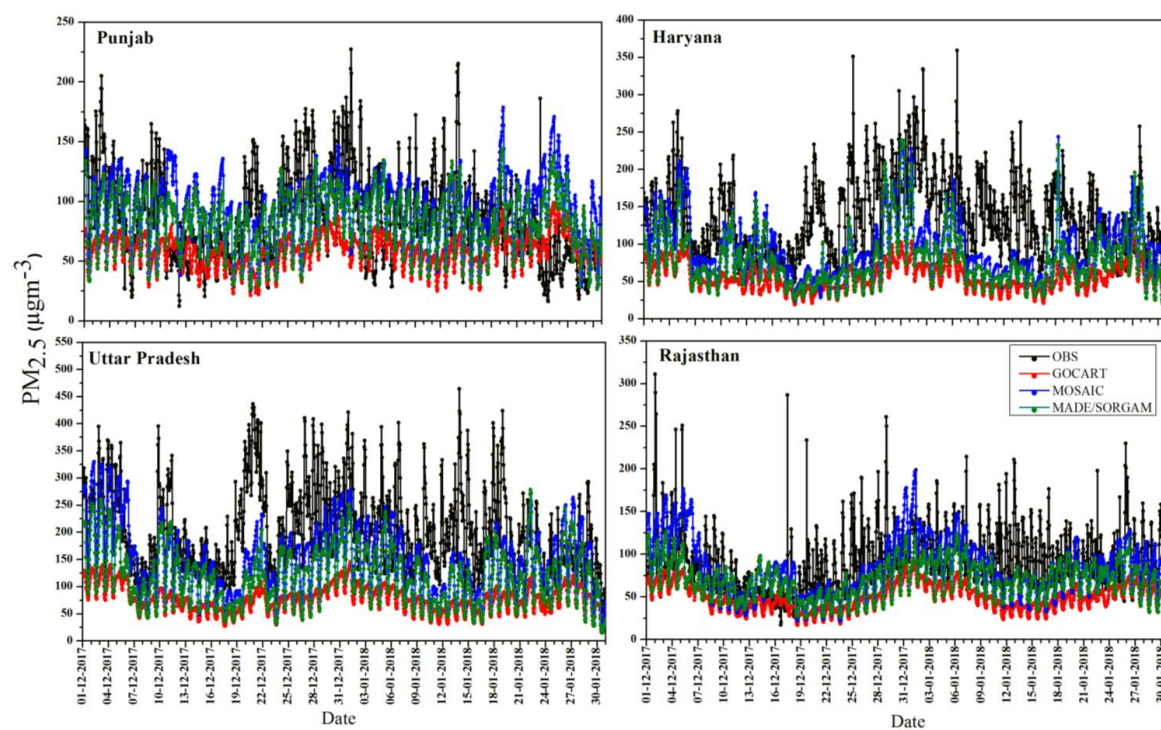




Figure 4:

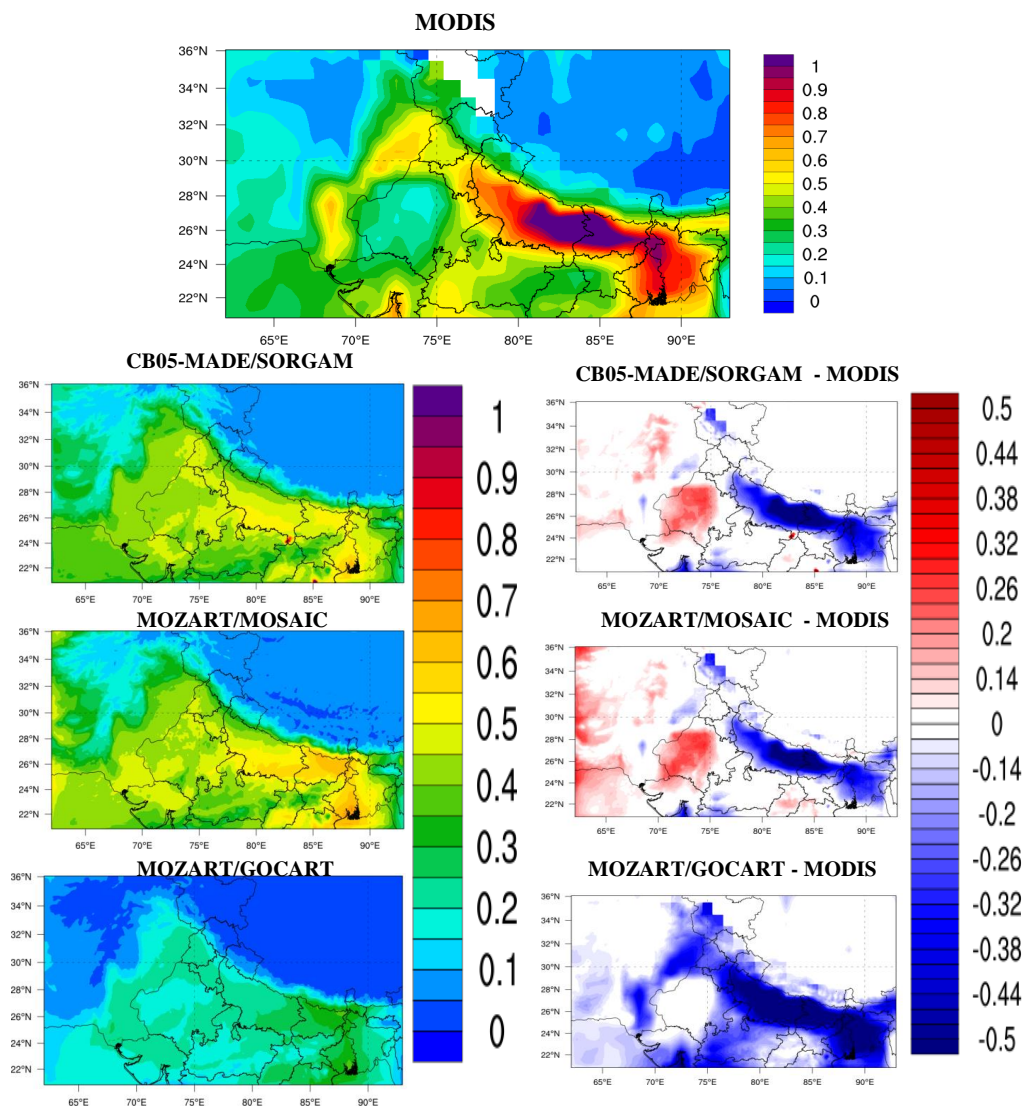




Figure 5:

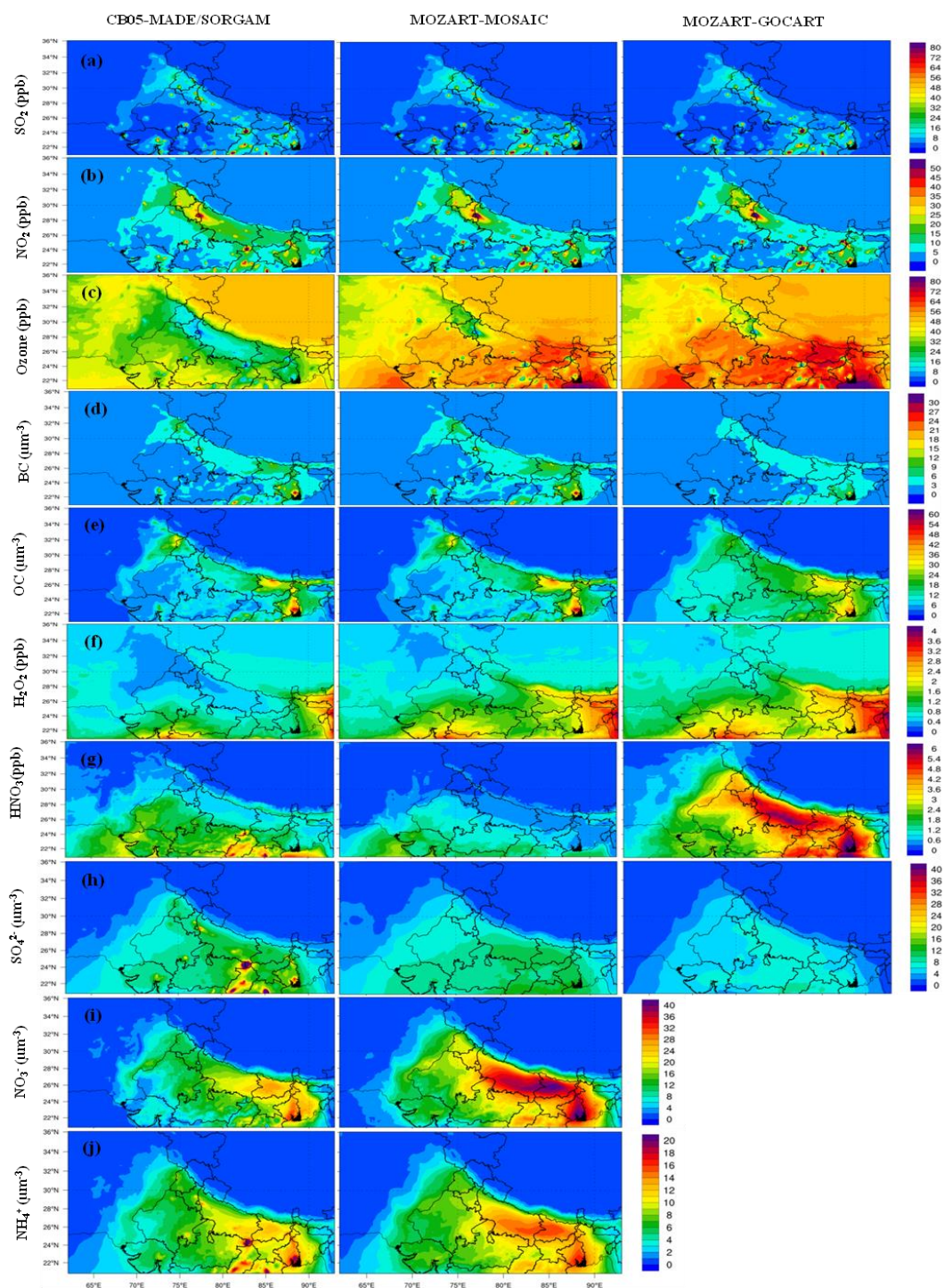




Figure 6:

IGI Airport T3, Delhi

